APPLICATIONS OF DETRENDED-FLUCTUATION ANALYSIS TO GEARBOX FAULT DIAGNOSIS

E. P. de Moura, elineudo@metalmat.ufc.br
A. P. Vieira, apvieira@metalmat.ufc.br
Departamento de Engenharia Metalúrgica e de Materiais, Universidade Federal do Ceará, 60455-760 Fortaleza, CE, Brazil

M. A. S. Irmão, marcos.silva@univasf.edu.br
Colegiado de Engenharia Mecânica, Universidade Federal do Vale do São Francisco, 48909-810, Juazeiro, BA, Brazil

A. A. Silva, almeida@dem.ufcg.edu.br
Departamento de Engenharia Mecânica, Universidade Federal de Campina Grande, 58109-970, Campina Grande, PB, Brazil

Abstract. *Aiming at fault diagnosis, we study vibration signals obtained from gearboxes under various conditions. We consider normal gearboxes, gearboxes containing scratched gears, and gearboxes containing toothless gears, both unloaded and under load, with several rotation frequencies. By applying detrended-fluctuation analysis (DFA), a mathematical tool introduced to study fractal properties of time series, we are able to distinguish the signals with respect to their working conditions. For each signal, DFA involves performing a linear fit to the data inside intervals of a certain size, and evaluating the corresponding fluctuations detrended by the local fit. Repeating this procedure for many interval sizes yields a curve of the average fluctuation as a function of size. From the curves, we define vectors whose components correspond to the average fluctuation associated with suitably chosen interval sizes. We finally apply principal component analysis to the set of all vectors, obtaining very good clustering of the transformed vectors according to the different working conditions, with at least the same performance obtained from Fourier analysis.*

Keywords: *Gearbox fault diagnosis, detrended-fluctuation analysis, principal-component analysis*

1. INTRODUCTION

Gearboxes are widely employed in industrial applications, lending great importance to studies aiming at gear-fault identification and characterization. The usual approach employed by those studies is to analyze vibration signals captured by an accelerometer mounted on the surface of the gear case. However, these are influenced by vibrations from many sources, such as the meshing gears, shafts, and bearings. Thus, the resulting signals are usually quite complex, hindering their analysis.

Many fault-detection techniques developed so far focus on the evolution of statistical parameters (such as standard deviation, skew, kurtosis, etc.) as a function of time (Li and Limmer, 2000), or in frequency analysis (Randall, 1982). More recently, a series of hybrid time-frequency techniques have been developed, such as wavelet, Wigner-Ville or correlated transforms (Wang and McFadden, 1993a, Wang and McFadden, 1993b, Wang and McFadden, 1996, Lin and Zuo, 2003, Padovese, 2004, Silva, Irmão and Padovese, 2006, Fan and Zuo, 2006). Both frequency and hybrid techniques rely on the identification of the frequencies present, which are then compared to models predicting which frequencies should be important in the presence of various faults.

Here we employ another approach, based on detrended-fluctuation analysis (DFA), a tool originally developed to differentiate between local patchiness and long-range correlations in DNA sequences (Peng et al., 1994). The presence of long-range correlations (which reflects the presence of correlated noise in the sequence) is identified by studying the detrended fluctuations in the sequence, as functions of the size of the windows through which the sequence is examined. In an analogous way, one may hope that DFA can be useful in investigations of vibration signals, by filtering out noise contributions from unimportant sources, and focusing on the correlated noise which presumably comes from the gear faults.

This paper is organized as follows. In section 2 we describe the techniques employed for producing and capturing the vibration signals. Section 3 details the motivation and mathematics behind detrended-fluctuation analysis. Results obtained from the combination of DFA and principal component analysis to the vibration signals are presented and discussed in section 4, and compared to a similar combination involving the Fourier spectra of the signals. Finally, section 5 contains our conclusions.

2. SIGNAL CAPTURE

All trials were performed on a specially designed bench, composed of a three-phase motor (with nominal power of 0.37 kW and nominal rotation frequency of 1555 rpm). Each gearbox contained four gears, but only the pinion gear was replaced by a damaged one.

The different types of gear studied were:

- gears with no faults (normal);
- gears with a local fault, represented by one missing tooth (toothless);
- gears with an extensive fault, represented by a severe scratch over ten consecutive teeth (scratched).

For each gear conditions, signals were captured using six different rotation frequencies (400 rpm, 600 rpm, 800 rpm, 1000 rpm, 1200 rpm, and 1400 rpm). The motor rotation was controlled by a frequency inverter. Trials were performed both in the absence of external load or under a load of 8.4 N $\cdot$ m, corresponding to 60% of the nominal maximum load.

For each combination of gear, frequency and load, 18 signals were captured, resulting in a data set composed of 648 samples of vibration signals. The capture made use of a B&K4393 accelerometer coupled to a B&K2535 load amplifier. Each signal is composed of 2048 data points, with a sampling rate of 5.12 kHz, and subjected to a low-pass filter with a 2 kHz cutoff.

3. DETRENDED-FLUCTUATION ANALYSIS

Most techniques of time series analysis focus on identifying properties of stationary signals (Chatfield, 1996), such as power spectra and autocorrelations, and assume any noise present in the signals to be non-correlated. By making use of concepts introduced in the study of fractional Brownian motion (fBm) (Addison, 1997), one can also study memory effects in the fluctuations of a time series, in order to identify the presence of correlated noise. In genuine fBm's these memory effects are embodied by a single number, the Hurst exponent H, which governs the time evolution of the standard deviation σ associated with the motion,

$$\sigma = (2K_f t)^H . \tag{1}$$

In the above equation, t is the time elapsed since the motion started, and K_f is a fractal diffusion coefficient. A Hurst coefficient equal to $\frac{1}{2}$ corresponds to a regular Brownian motion (i.e. Fickian diffusion), and to the absence of memory effects. Values of H different from $\frac{1}{2}$ indicate the presence of long-range memory mechanisms affecting the motion; $H > \frac{1}{2}$ ($H < \frac{1}{2}$) correspond to persistent (antipersistence) behavior of the time series.

The detrended-fluctuation analysis (DFA) (Peng et al. 1994) can be used a means of estimating the Hurst exponent of a time series by eliminating trends which could be superposed to an underlying fBm. The method consists initially in obtaining from the original series z_i (containing L points) a new integrated series $\tilde{z}_i$,

$$\tilde{z}_i = \sum_{k=1}^{i} \left(z_k - \langle z \rangle \right), \tag{2}$$

the average $\langle z \rangle$ being taken over all points,

$$\langle z \rangle = \frac{1}{L} \sum_{i=1}^{L} z_i. \tag{3}$$

After dividing the series into intervals, the points inside a given interval are fitted by a straight line. Then, a detrended variation function Δ_i is obtained by subtracting from the integrated data the local trend as given by the fit. Explicitly, we define

$$\Delta_i = \tilde{z}_i - h_i, \tag{4}$$

where h_i is the value associated with point i according to the linear fit. Finally, we calculate the root-mean-square fluctuation $F(\tau)$ inside an interval as

$$F(\tau) = \sqrt{\frac{1}{\tau} \sum_{i} \Delta_{i,n}^2}, \tag{5}$$

and average over all intervals. Usually $F(\tau)$ behaves as

$$F(\tau) \sim \tau^{\alpha}, \tag{6}$$

at least inside some τ interval, and the scaling exponent α provides an estimate of the Hurst exponent of the underlying fBm.

On the other hand, from a signal-processing point of view, DFA can be seen as a transformation yielding the function $F(\tau)$, which compresses the information content of the time series into a much smaller number of variables. (In the case of the vibration signals considered here, each original series contains 2048 points, whereas the corresponding $F(\tau)$ curves were calculated for a maximum of 37 values of τ.) The curves $F(\tau)$ representing the various working conditions can then be used in conjunction with statistical tools aiming at pattern classification.

Table 1. Number of misclassifications using the DFA approach with three principal components and the nearest-class-mean rule. The total number of points is 54 for all frequencies.

	400 rpm	600 rpm	800 rpm	1000 rpm	1200 rpm	1400 rpm
unloaded	11	2	0	14	6	8
loaded	1	0	0	1	1	0

Table 2. Number of misclassifications using the power-spectrum approach with three principal components and the nearest-class-mean rule. The total number of points is 54 for all frequencies.

	400 rpm	600 rpm	800 rpm	1000 rpm	1200 rpm	1400 rpm
unloaded	10	1	0	0	1	4
loaded	0	0	0	0	0	0

4. RESULTS AND DISCUSSION

Figure 1 shows representative signals obtained from the three types of gear, working under load at a rotation frequency of 1400 rpm. Also shown are the corresponding DFA curves. The detrended-fluctuation analysis was performed by selecting a fixed set $\{\tau_j\}$ of values of the window size τ, ranging from 2 to 2048 time steps, and calculating for each signal i the values $F(\tau_j)$. These values can be interpreted as the components of a vector $\mathbf{x}_i$. The window sizes we used for the vectors correspond to $\{4, 5, 6, 7, 8, 10, 11, 13, 16, 19, 23, 27, 32\}$, so that each vector has 13 components (other choices of the window sizes lead to similar results). We then grouped the resulting vectors according to the rotation frequency and to the presence or absence of load, and applied principal component analysis (PCA) (Webb, 2002) to each group. As widely known, PCA works by projecting the vectors onto the directions defined by the eigenvectors of the group covariance matrix. The projection in the direction of the eigenvector corresponding to the largest eigenvalue is the first principal component, and is expected to account for the largest amount of variation in the original vectors. The remaining principal components are arranged in decreasing order of the corresponding eigenvalues.

Figures 2 and 3 show plots of the second versus the first principal components calculated from the DFA results obtained for all studied rotation frequencies, both in the absence and in the presence of external load. For the unloaded signals (Fig. 2), all frequencies allow for a clear discrimination of the signals obtained from scratched gears, although the points corresponding to normal and toothless gears are hardly distinguishable from just the first two components. On the other hand, under load (Fig. 3) a much clearer distinction is established between the three classes of gear, especially for higher frequencies.

In order to make a quantitative assessment of the quality of the discrimination obtained from the DFA approach, we determined the average vectors of each class, for each group, using the first three principal components, and classified the different vectors within the same group according to the nearest-class-mean rule (i.e., a vector $\mathbf{x}$ is assigned to the class whose average vector lies closer to $\mathbf{x}$). Table 1 shows results for the number of misclassifications obtained by following this approach, for all groups of signals (each containing 18 vectors belonging to each class, with a total of 54). In the absence of load, the number of misclassifications is at most 14 (which occurs for a rotation frequency 1000 rpm), corresponding to a relative error of 26%; for other rotation frequencies, the error can be much lower, reaching zero for 800 rpm. In the presence of load, which corresponds to the most common operating condition, the relative error drops to at most 2%, with only one misclassification occurring in three of the groups, and none in the remaining ones.

The performance of the DFA approach is comparable, although slightly inferior, to that obtained by combining calculations of the power spectrum of the signals with PCA. Analogously to the DFA approach, we fixed the FFT frequencies $\{\omega_j\}$, and defined for each signal i a vector $\mathbf{y}_i$ whose components are $P(\omega_j)$, the power spectral density associated with frequency ω_j. Since each time signal has 2048 points, each FFT vector has 1024 components. Results for this combination are shown in Figs. 4 and 5. Again, in the absence of load (Fig. 4), points corresponding to scratched gears are clearly distinct from those of the other two classes of gear, which are rather indistinct. Under load (Fig. 5), however, the three classes are more easily distinguishable, and for lower frequencies than in the DFA case. Table 2 shows the number of misclassifications obtained by applying the nearest-class-mean rule with the first three principal components of the FFT. For the unloaded signals, the performance is clearly superior to that of the DFA approach. For the loaded signals, no misclassification errors occur, while in the DFA approach the error rate was very low, although nonzero. Notice, however, that in DFA approach the information of all 2048 points in each signal was compressed in only 13 vector components, but the discriminating power was almost fully preserved for the loaded signals.

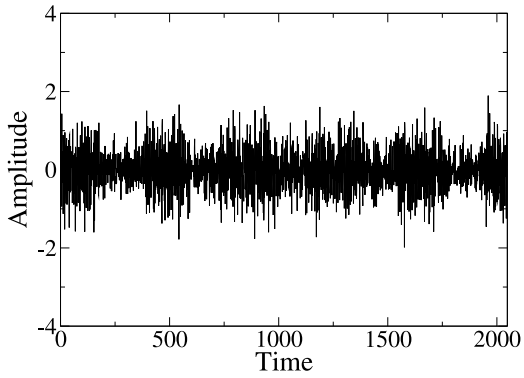

(a) Signal from normal gear

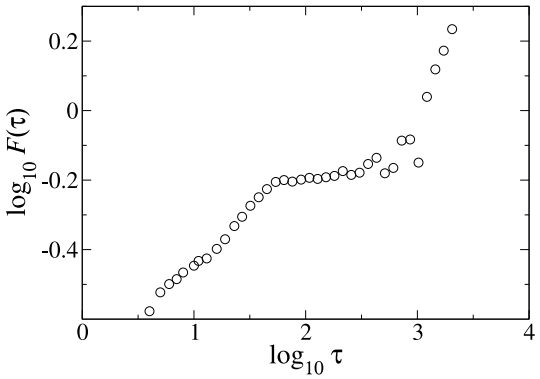

(b) DFA from normal gear

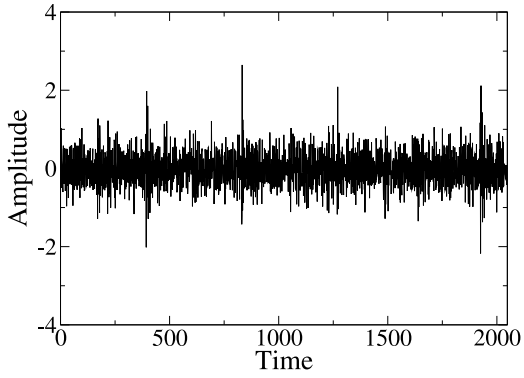

(c) Signal from toothless gear

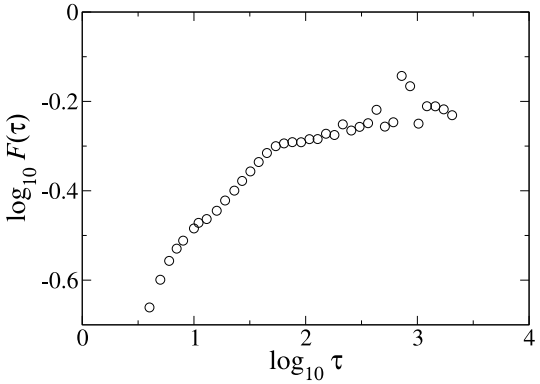

(d) DFA from toothless gear

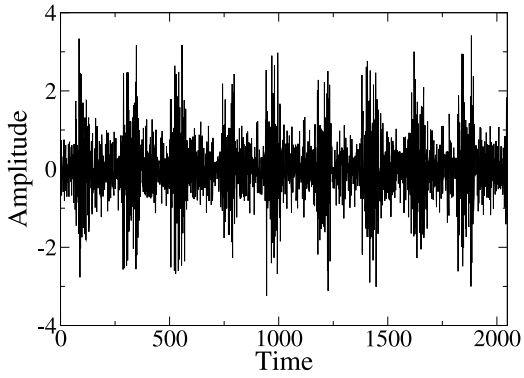

(e) Signal from scratched gear

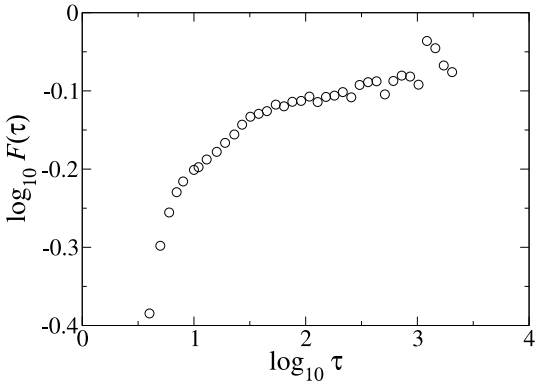

(f) DFA from scratched gear

Figure 1. Representative signals and DFA curves obtained from the three types of gear, working under load at a rotation frequency of 1400 rpm. In the signal plots, time is measured in units of the inverse sampling rate.

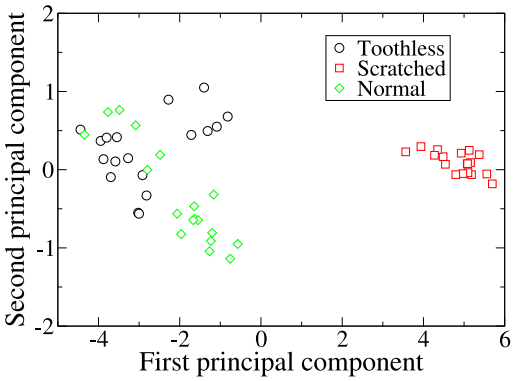

(a) 400 rpm

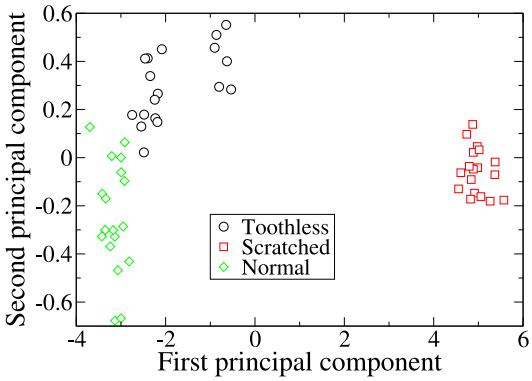

(b) 600 rpm

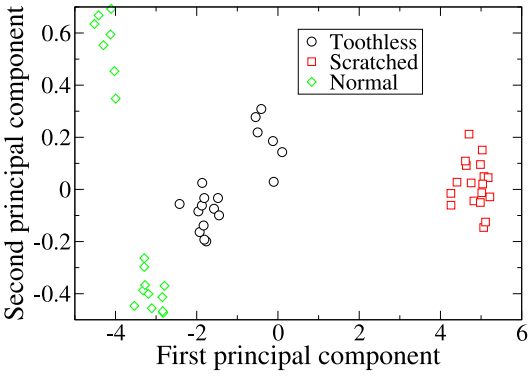

(c) 800 rpm

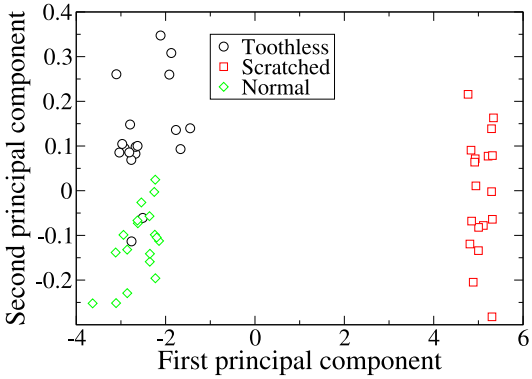

(d) 1000 rpm

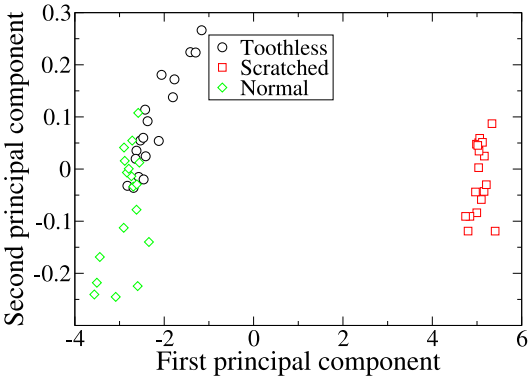

(e) 1200 rpm

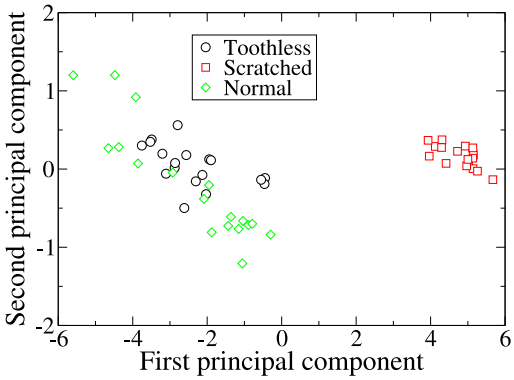

(f) 1400 rpm

Figure 2. DFA, unloaded.

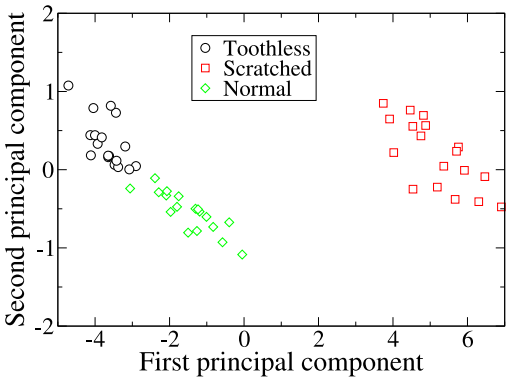

(a) 400 rpm

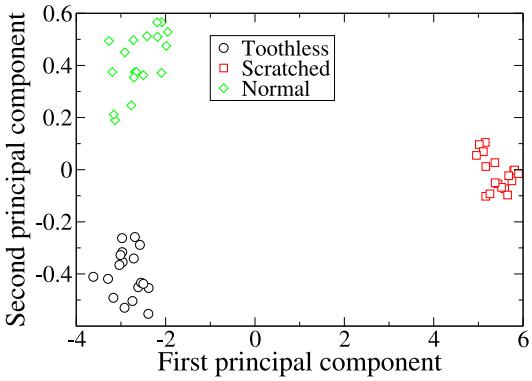

(b) 600 rpm

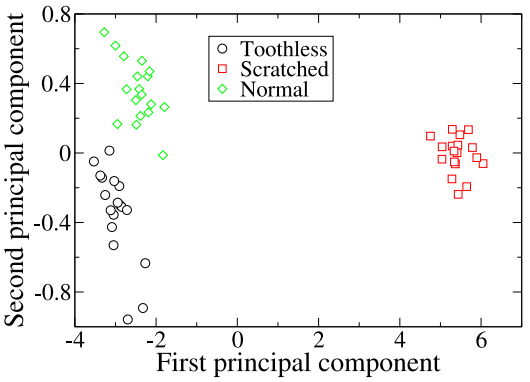

(c) 800 rpm

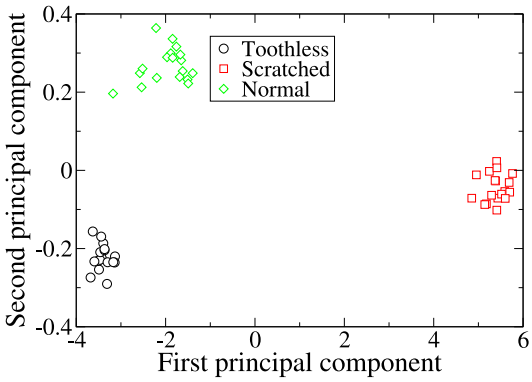

(d) 1000 rpm

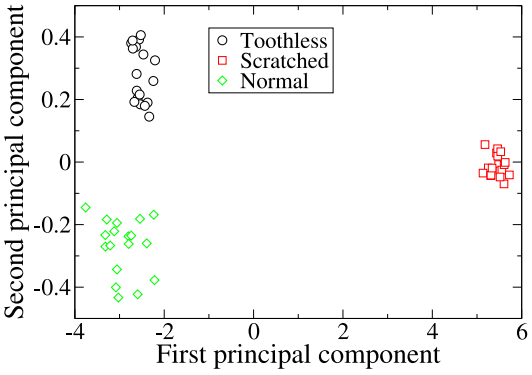

(e) 1200 rpm

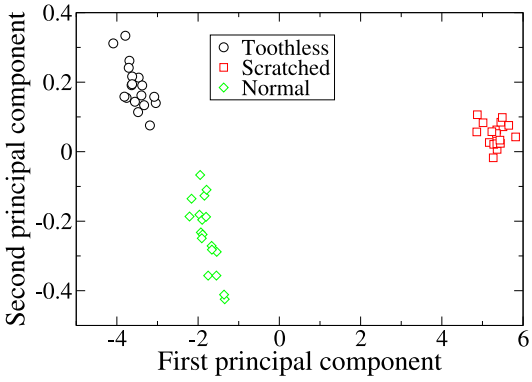

(f) 1400 rpm

Figure 3. DFA, loaded.

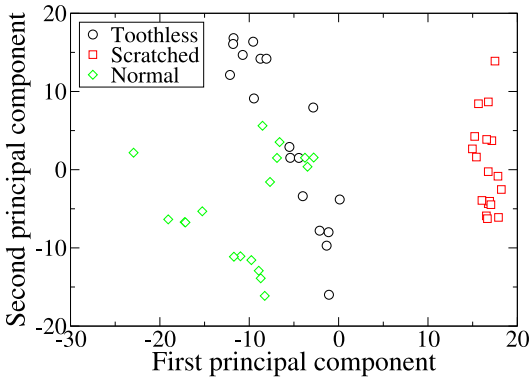

(a) 400 rpm

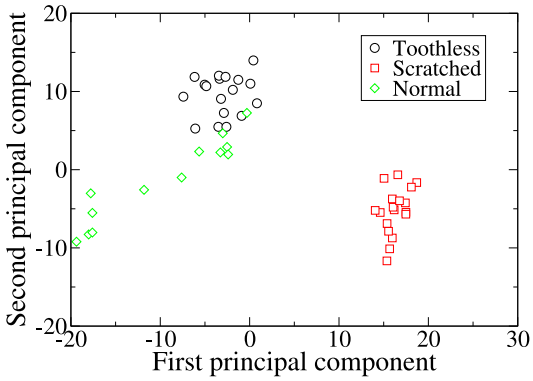

(b) 600 rpm

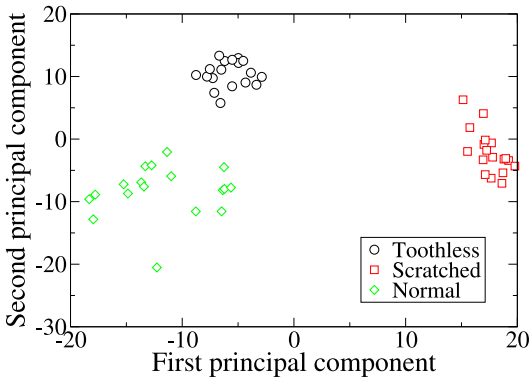

(c) 800 rpm

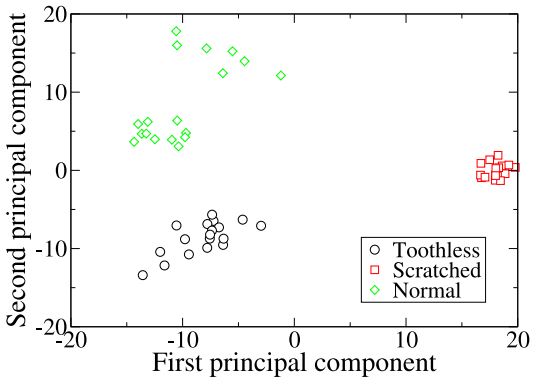

(d) 1000 rpm

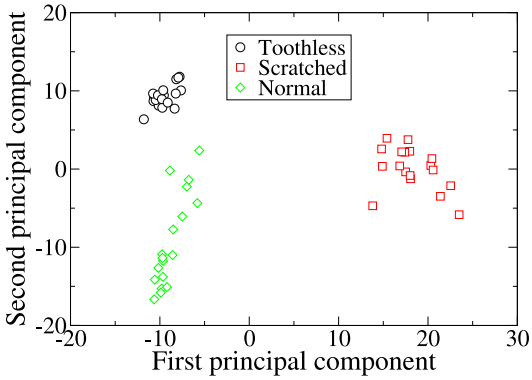

(e) 1200 rpm

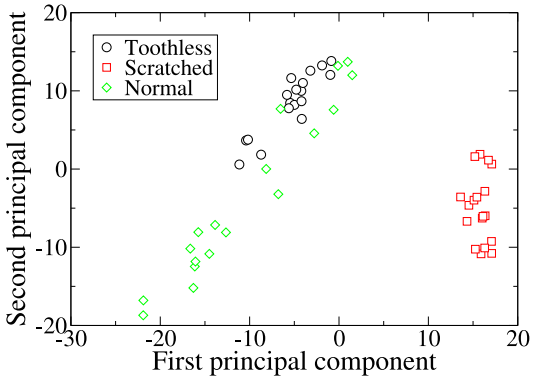

(f) 1400 rpm

Figure 4. Power spectrum, unloaded.

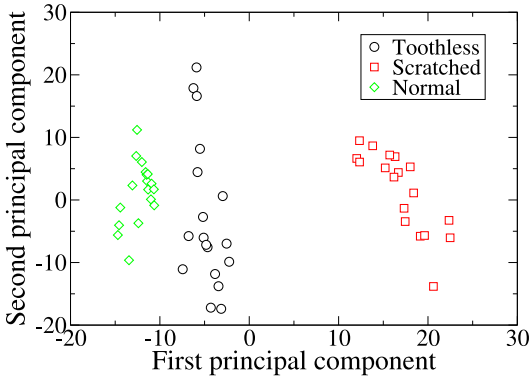

(a) 400 rpm

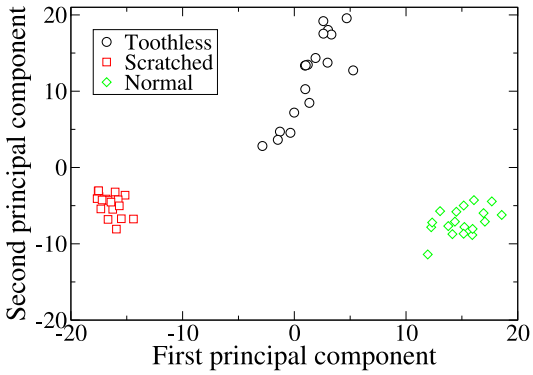

(b) 600 rpm

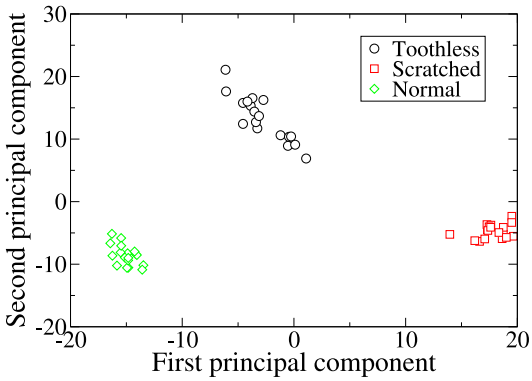

(c) 800 rpm

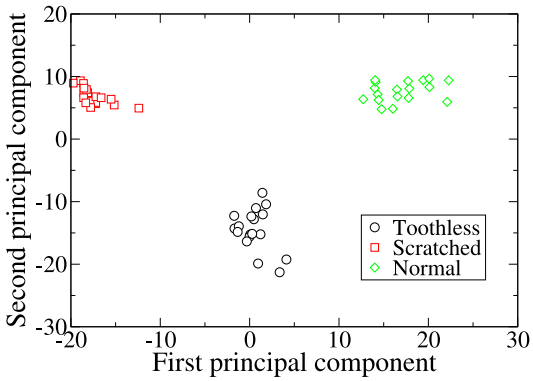

(d) 1000 rpm

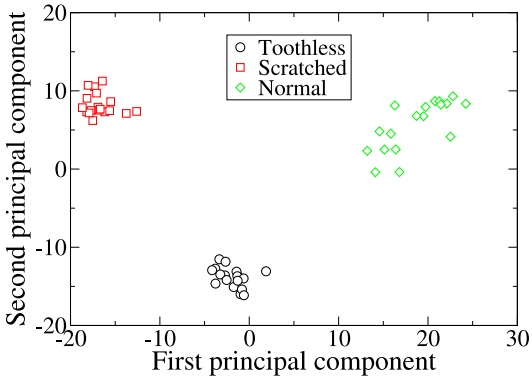

(e) 1200 rpm

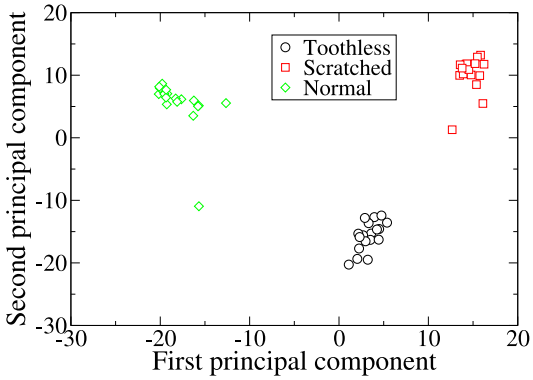

(f) 1400 rpm

Figure 5. Power spectrum, loaded.

5. CONCLUSIONS

We applied a combination of detrended-fluctuation analysis (DFA) and principal component analysis (PCA) to discriminate between vibrational signals obtained from three classes of gears (normal, toothless, and scratched), under various working conditions. The performance of the method was only slightly inferior to that provided by a similar approach based on power-spectrum analysis, but with the advantage of employing a significantly smaller set of variables. Owing to the nature of the detrended-fluctuation analysis, we believe that the DFA+PCA approach could be a quite useful tool also in the case of nonstationary signals, in which power-spectrum approaches are hardly expected to provide sensible results.

6. ACKNOWLEDGMENTS

This work was partially financed by CNPq and FUNCAP.

7. REFERENCES

Addison, P. S., 1997, "Fractals and Chaos", IOP, London.

Chatfield, C., 1996, "The Analysis of Time Series", 5th Ed., Chapman & Hall/CRC, Boca Raton.

Fan, X. and Zuo, M. J., 2006, "Gearbox fault detection using Hilbert and wavelet packet transform", Mech. Syst. Signal Process., Vol. 20, pp. 966–982.

Li, C. J. and Limmer, J. D., 2000, "Model-based condition index for tracking gear wear and fatigue damage", Wear, Vol. 241, pp. 26–32.

Lin, J. and Zuo, M. J., 2003, "Gearbox fault diagnosis using adaptive wavelet filter", Mech. Syst. Signal Process., Vol. 17, pp. 1259–1269.

Padovese, L. R., 2004, "Hybrid time-frequency methods for nonstationary mechanical signals", Mech. Syst. Signal Process., Vol. 18, pp. 1047–1064.

Peng, C. K., Buldyrev, V., Havlin, S., Simmons, M., Stanley, H. E. and Goldberger, A. L., 1994, "Mosaic organization of DNA nucleotides", Phys. Rev. E, Vol. 49, pp. 1685–1689.

Randall, R. B., 1982, "A new method of modeling gear faults", J. Mech. Design, Vol. 104, pp. 259–267.

Silva, A. A., Irmão, M. A. and Padovese, L. R.: 2006, "Otimização de representações tempo-freqüência na análise de falhas em sistemas engrenados", Revista Iberoamericana de Ingeniería Mecánica, Vol. 10, pp. 35–45.

Wang, W. J. and McFadden, P. D., 1993a, "Early detection of gear failure by vibration analysis .1. Calculation of the time-frequency distribution", Mech. Syst. Signal Process., Vol. 7, pp. 193–203.

Wang, W. J. and McFadden, P. D., 1993b, "Early detection of gear failure by vibration analysis .2. Interpretation of the time-frequency distribution using image-processing techniques", Mech. Syst. Signal Process., Vol. 7, pp. 205–215.

Wang, W. J. and McFadden, P. D., 1996, "Application of wavelets to gearbox vibration signals for fault detection", Journal of Sound and Vibration Vol. 192, pp. 927–939.

Webb, A. R., 2002, "Statistical Pattern Recognition", 2nd ed., John Wiley & Sons, West Sussex.